LIDAR-DERIVED ELEVATION DATA FOR BARRY ARM LANDSLIDE, SOUTHCENTRAL ALASKA, OCTOBER 16, 2020

Katreen M. Wikstrom Jones, Gabriel J. Wolken, and Ronald P. Daanen

Raw Data File 2026-5

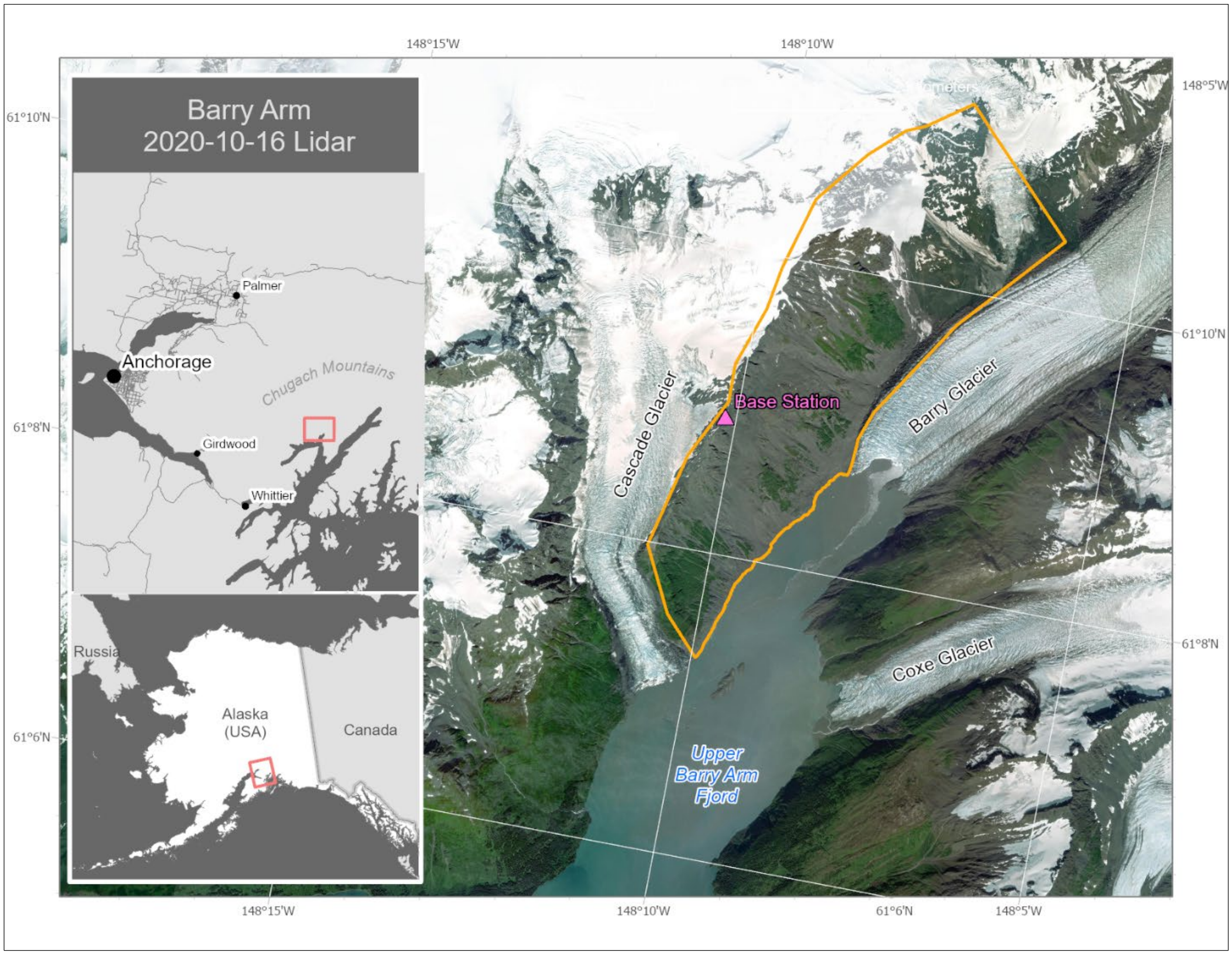

Location map of the survey area with an orthometric image.

This report has not been reviewed for technical content or for conformity to the editorial standards of DGGS

2026
STATE OF ALASKA
DEPARTMENT OF NATURAL RESOURCES
DIVISION OF GEOLOGICAL & GEOPHYSICAL SURVEYS

STATE OF ALASKA
Mike Dunleavy, Governor

DEPARTMENT OF NATURAL RESOURCES
John Crowther, Commissioner-Designee

DIVISION OF GEOLOGICAL & GEOPHYSICAL SURVEYS
Erin A. Campbell, State Geologist & Director

Publications produced by the Division of Geological & Geophysical Surveys are available to download from the DGGS website (dggs.alaska.gov). Publications on hard-copy or digital media can be examined or purchased in the Fairbanks office:

Alaska Division of Geological & Geophysical Surveys (DGGS)
3354 College Road | Fairbanks, Alaska 99709-3707
Phone: 907.451.5010 | Fax 907.451.5050
dggspubs@alaska.gov | dggs.alaska.gov

DGGS publications are also available at:

Alaska State Library, Historical
Collections & Talking Book Center
395 Whittier Street
Juneau, Alaska 99801

Alaska Resource Library and
Information Services (ARLIS)
3150 C Street, Suite 100
Anchorage, Alaska 99503

Suggested citation:
Wikstrom Jones, K.M., Wolken, G.J., and Daanen, R.P., 2026, Lidar-derived elevation data for Barry Arm landslide, southcentral Alaska, October 16, 2020: Alaska Division of Geological & Geophysical Surveys Raw Data File 2026-5, 9 p.
https://doi.org/10.14509/31970

LIDAR-DERIVED ELEVATION DATA FOR BARRY ARM LANDSLIDE, SOUTHCENTRAL ALASKA, OCTOBER 16, 2020

Katreen M. Wikstrom Jones[1], Gabriel J. Wolken[1], and Ronald P. Daanen[1*]

INTRODUCTION

The Alaska Division of Geological & Geophysical Surveys (DGGS) used aerial lidar to produce a classified point cloud, a digital terrain model (DTM), a surface model (DSM), and an intensity model for the Barry Arm landslide, northeast of Whittier in Prince William Sound in southcentral Alaska, during near-snow-free ground conditions. The goal of the survey is to provide snow-free surface elevation data to assess landslide movement using repeat surveys during snow-free conditions. Airborne data were collected on October 16, 2020, and subsequently processed in Terrasolid and ArcGIS. Ground control was also collected on October 16, 2020. These data are provided as a Raw Data File under an open end-user license and are available on the DGGS website (http://doi.org/10.14509/31970).

LIST OF DELIVERABLES

- Classified Points
- DSM, DTM, and hydro-enforced DTM
- Intensity Image
- Metadata

MISSION PLAN

Aerial Lidar Survey Details

DGGS used a Riegl VUX1-LR laser scanner with a global navigation satellite system (GNSS) and a Northrop Grumman LN-200C inertial measurement unit (IMU) integrated by Phoenix LiDAR Systems. The sensor can collect a maximum of 820,000 points per second at a range of 215 m, or a minimum of 50,000 points per second at 820 m (ranges assume ≥ 20 percent natural reflectance). This survey was flown with a pulse refresh rate of 200,000 to 400,000 pulses per second and a scan rate of 80 to 150 lines per second. We used a Cessna 180 Skywagon fixed-wing platform to survey from an elevation of approximately 100–300 m above ground level, at a ground speed of approximately 40 m/s, and with a scan angle set from 80 to 280 degrees. The total area surveyed was approximately 12.6 km^2 (outlined in red in the cover figure).

Weather Conditions and Flight Times

The airborne survey was flown on October 16, 2020, beginning at 9:35 am AKST and ending at 10:48 am AKST (fig. 1). The weather throughout the survey was fair and cloudless.

1Alaska Division of Geological & Geophysical Surveys, 3354 College Road, Fairbanks, AK 99709
*Former DGGS, in memoriam

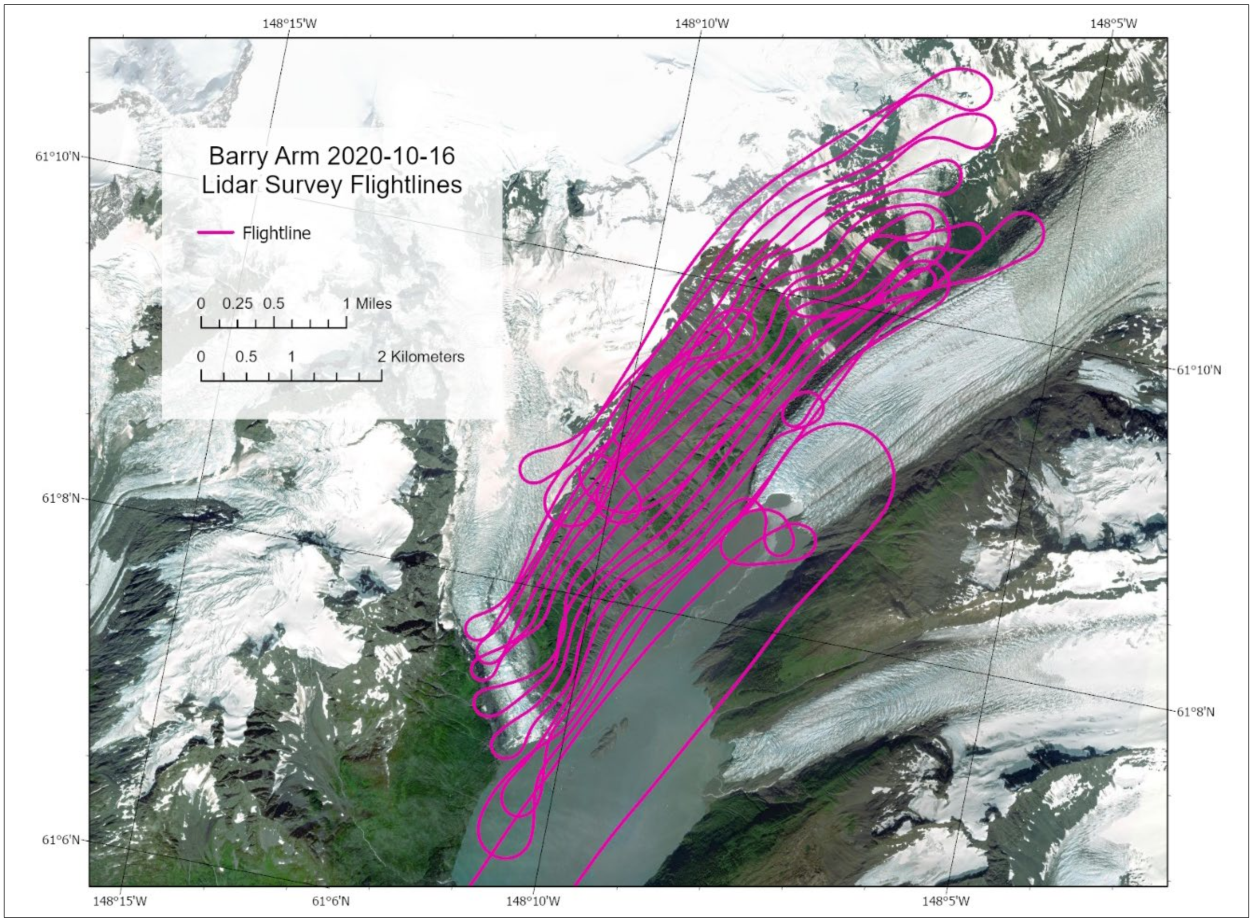

Figure 1. Lidar data collection flightlines.

PROCESSING REPORT

Lidar Dataset Processing

We processed point data in SDCimport for initial filtering and multiple-time-around (MTA) disambiguation. MTA errors, corrected in this process, result from ambiguous interpretations of received pulse time intervals and occur more frequently with higher pulse refresh rates. IMU and GNSS data were processed in Inertial Explorer, and flightline information was integrated with the point cloud in Spatial Explorer. We calibrated the point data at an incrementally precise scale of sensor movement and behavior, incorporating sensor velocity, roll, pitch, and yaw fluctuations throughout the survey. For the lidar data collection, the pulse density is 41.3 pulses/m^2, and the average pulse spacing is 15.6 cm.

We created a macro (an ordered list of point classification commands tailored to this dataset) in Terrasolid software and classified points in accordance with the American Society for Photogrammetry & Remote Sensing (ASPRS) 2025 guidelines (ASPRS, 2025). After classification, we applied a geometric transformation to convert points from ellipsoidal heights to GEOID12B (Alaska) orthometric heights.

Raster products were derived from the point cloud in ArcGIS Pro. A 20-cm DSM was interpolated from ground and vegetation classes using a triangulation method and maximum values. A 20-cm DTM was interpolated from all ground-class returns using triangulation method and minimum values. We also produced a 1-m intensity image for the area using average binning in ArcGIS Pro, with no normalization or corrections applied.

Classified Point Cloud

Classified point cloud data are provided in LAZ format. Data are classified according to the ASPRS 2025 guidelines (table 1) and include return and intensity information. For classified ground points, the average point density is 32.1 pts/m^2, and the average spacing is 17.6 cm (fig. 2).

Table 1. Point cloud class code definitions.

Class Code	Description
1	Unclassified
2	Ground
3	Low Vegetation, ≥ 0.0m, < 0.5m
4	Medium Vegetation, ≥ 0.5m, < 3m
5	High Vegetation, ≥ 3m
7	Low Noise
18	High Noise

Digital Surface Model

The DSM represents surface elevations, including the heights of vegetation, buildings, power lines, pipes, and bridge decks. The overall DSM is a single-band, 32-bit GeoTIFF file of 50-cm resolution. No Data value is set to -3.40282306074e+38 (32-bit, floating-point minimum).

Digital Terrain Model

The DTM represents bare-earth elevations, excluding vegetation, bridge decks, buildings, and similar features. The overall DTM is a single-band, 32-bit GeoTIFF file of 50-cm resolution. No Data value is set to -3.40282306074e+38.

Lidar Intensity Image

The lidar intensity image describes the relative amplitude of reflected signals contributing to the point cloud. Lidar intensity is (1) primarily a function of scanned object reflectance in relation to the signal frequency, (2) dependent on ambient conditions, and (3) not necessarily consistent between separate scans. The intensity image is a single-band, 32-bit GeoTIFF file of 1-m resolution. No Data value is set to -3.40282306074e+38.

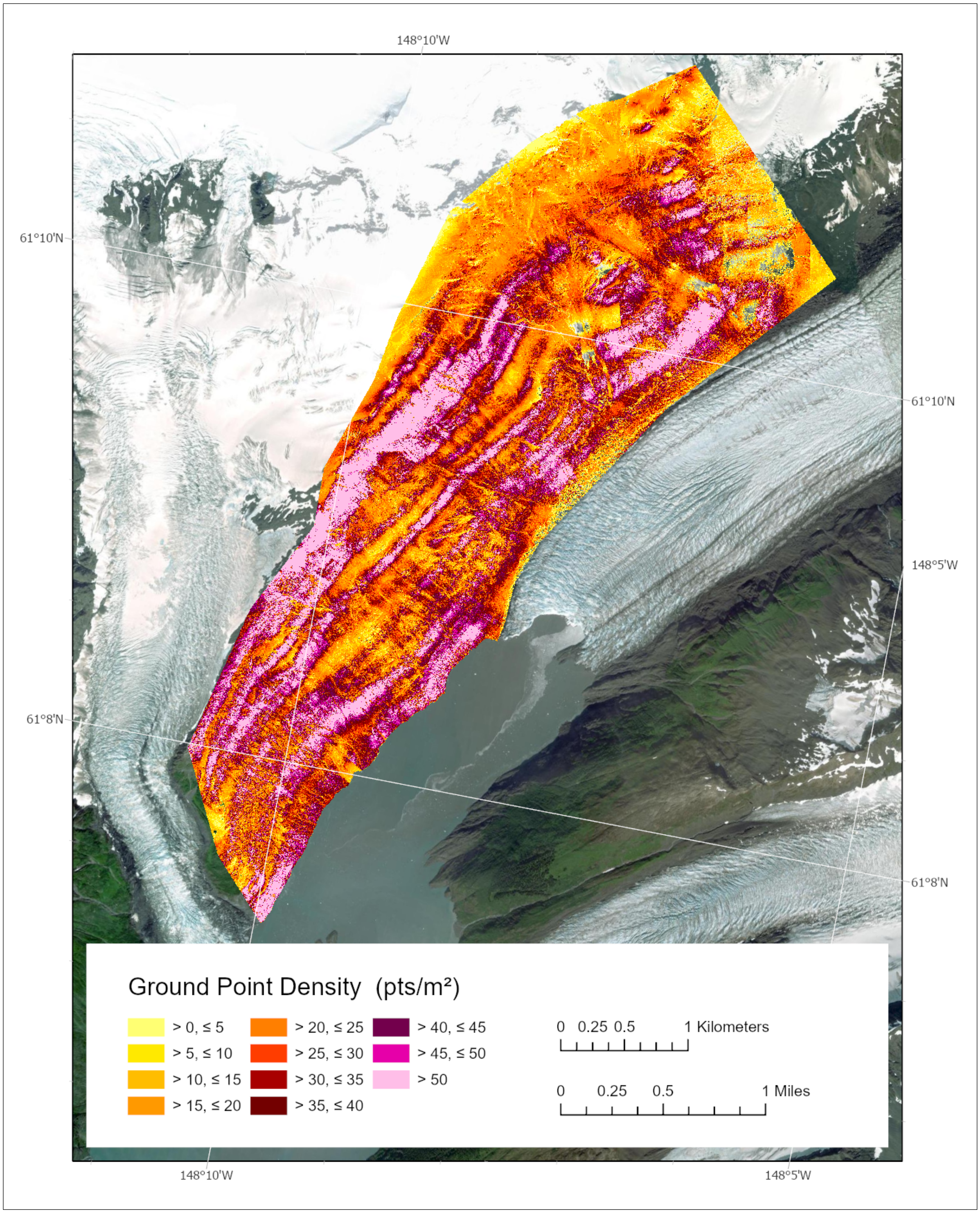

Figure 2. Ground point density for the survey displayed as a raster.

SURVEY REPORT

Ground Survey Details

Ground control and checkpoints were collected on October 16, 2020. A Trimble R10-2 GNSS receiver with an internal antenna was deployed near the center of the study area on the ridge. It provided a base station occupation and real-time kinematic (RTK) corrections to points surveyed with a rover Trimble R10-2 GNSS receiver (internal antenna). We collected 70 ground control and check points to use for calibration and to assess the vertical accuracy of the point cloud; 67 of these were used for this lidar acquisition. Checkpoints were collected on bare earth or minimally vegetated surface.

Coordinate System and Datum

We processed and delivered all data in NAD83 (2011), UTM zone 6N, and vertical datum NAVD 88 (GEOID12B).

Horizontal Accuracy

Horizontal accuracy was not measured for this collection; it is considered inherent in the airborne GPS/IMU solution.

Vertical Accuracy

We measured a vertical mean offset of +77.2 cm between 54 control points and the point cloud (app. 1). This offset was reduced to -3 cm by applying a constant vertical correction to the lidar point data. We used 15 checkpoints to determine the non-vegetated vertical accuracy (NVA) of the point cloud ground class, using a tin-based approach. Project NVA was calculated to have a root mean square error (RMSE) of 20 cm (app. 2). Relative accuracy was evaluated based on interswath overlap consistency, yielding an RMSE of 2.3 cm.

Data Consistency and Completeness

This is a full-release dataset. There was no over-collect. Data quality is consistent throughout the survey, save for gaps over bodies of water, glaciers, and snow-covered surfaces.

ACKNOWLEDGMENTS

These data products were funded by the State of Alaska Landslide Hazard Capital Improvement Project and collected and processed by DGGS. We thank Clearwater Air and Alpine Air for their aviation expertise and contribution to these data products.

REFERENCES

The American Society for Photogrammetry & Remote Sensing (ASPRS), 2025, LAS Specification 1.4 - R16. https://publicdocuments.asprs.org/las-v14-r16-2025

APPENDIX 1: GROUND CONTROL POINTS

GCP	Easting (m)	Northing (m)	Known Z (m)	Laser Z (m)	Dz (m)
1	437057.306	6779902.245	1093.012	1093.53	0.518
2	437056.598	6779914.767	1093.439	1094.03	0.591
3	437053.779	6779911.615	1093.732	1094.33	0.598
4	437055.584	6779877.015	1091.967	1092.55	0.583
5	437052.335	6779845.423	1095.76	1096.4	0.64
6	437051.613	6779823.287	1097.279	1097.79	0.511
7	437033.34	6779815.469	1096.543	1097.15	0.607
8	437045.47	6779779.207	1088.057	1088.74	0.683
9	437013.162	6779735.137	1087.01	1087.32	0.31
10	437006.044	6779719.831	1084.907	1085.39	0.483
11	437040.848	6779815.481	1096.467	1096.93	0.463
12	437061.824	6779878.572	1091.116	1091.74	0.624
13	437062.781	6779887.832	1091.204	1091.81	0.606
14	437058.059	6779887.397	1092.381	1092.95	0.569
15	436747.268	6777536.287	579.766	580.66	0.894
16	436756.951	6777542.325	582.421	583.41	0.989
17	436772.365	6777549.261	586.171	587.18	1.009
18	436778.738	6777568.239	585.053	586.07	1.017
19	436793.786	6777566.505	590.02	590.96	0.94
20	436800.598	6777571.027	590.35	591.3	0.95
21	436788.591	6777577.344	586.391	587.4	1.009
22	436795.133	6777583.579	588.243	589.22	0.977
23	436784.168	6777588.298	584.505	585.47	0.965
24	436774.452	6777581.158	582.765	583.69	0.925
25	436762.172	6777581.653	580.473	581.44	0.967
26	436761.525	6777588.367	580.744	581.7	0.956
27	436737.412	6777600.878	580.375	581.24	0.865
28	436733.825	6777606.857	581.695	582.61	0.915
29	436713.849	6777597.916	574.918	575.87	0.952
30	436704.768	6777606.804	575.304	576.25	0.946
31	436689.565	6777612.095	578.405	579.32	0.915
32	436721.092	6777581.615	571.954	572.9	0.946
33	436728.418	6777584.597	571.838	572.78	0.942
34	436733.905	6777570.248	572.184	573.11	0.926
35	437605.917	6779349.297	544.519	545.32	0.801
36	437604.964	6779346.102	544.633	545.45	0.817
37	437613.731	6779351.104	545.133	545.81	0.677
38	437619.695	6779352.415	545.724	546.42	0.696
39	437612.287	6779336.922	546.606	547.26	0.654
40	437607.225	6779334.216	544.952	545.74	0.788
41	437613.925	6779348.229	546.19	546.95	0.76

42	437593.037	6779364.1	549.98	550.78	0.8
43	437586.902	6779372.316	550.304	551.05	0.746
44	437583.234	6779374.449	551.09	551.76	0.67
45	437579.957	6779375.442	551.262	552.04	0.778
46	437575.198	6779376.18	553.017	553.64	0.623
47	437568.457	6779371.298	555.437	556.21	0.773
48	437564.13	6779373.497	556.284	557.01	0.726
49	437558.409	6779367.633	558.266	558.98	0.714
50	437556.192	6779361.344	558.377	559.18	0.803
51	437553.318	6779357.885	559.155	559.91	0.755
52	437544.654	6779358.795	560.285	561.07	0.785
53	437541.084	6779357.815	560.819	561.55	0.731
54	437535.761	6779350.997	561.759	562.57	0.811
Average dz (m)	0.772				
Minimum dz (m)	0.31				
Maximum dz (m)	1.017				
Average magnitude error (m)	0.772				
Root mean square error (m)	0.79				
Standard deviation (m)	0.169				

APPENDIX 2: CHECKPOINTS

GCP	Easting (m)	Northing (m)	Known Z (m)	Laser Z (m)	Dz (m)
1	437057.1	6779890.5	1092.643	1092.43	-0.213
2	437059.5	6779884.8	1092.156	1092.09	-0.066
3	437045.7	6779783.1	1087.317	1087.18	-0.137
4	436985.5	6779684	1084.02	1083.65	-0.37
5	437057.5	6779912.6	1093.943	1093.68	-0.263
6	436790.6	6777561	590.877	591.14	0.263
7	436808.4	6777577.5	589.495	589.82	0.325
8	436748.7	6777583.6	577.988	578.14	0.152
9	436685.3	6777622.6	578.601	578.74	0.139
10	436723.5	6777538.8	572.876	573.03	0.154
11	437621.5	6779345.3	547.279	547.01	-0.269
12	437589.1	6779374.5	549.769	549.69	-0.079
13	437571.4	6779371.8	554.454	554.39	-0.064
14	437555.5	6779359.5	558.805	558.77	-0.035
15	437536.8	6779358.2	562.25	562.26	0.01
Average dz (m)	-0.03				
Minimum dz (m)	-0.37				
Maximum dz (m)	0.325				
Average magnitude error (m)	0.169				
Root mean square error (m)	0.2				
Standard deviation (m)	0.205				

In Memoriam
Ronald P. Daanen